

1 Title: **The mammalian cervical vertebrae blueprint depends on the T (*brachyury*) gene**

2

3 Andreas Kromik<sup>\*</sup>, Reiner Ulrich<sup>§</sup>, Marian Kusenda<sup>†</sup>, Andrea Tipold<sup>‡</sup>, Veronika M. Stein<sup>‡</sup>,  
4 Maren Hellige<sup>\*\*</sup>, Peter Dziallas<sup>‡</sup>, Frieder Hadlich<sup>\*</sup>, Philipp Widmann<sup>\*</sup>, Tom Goldammer<sup>\*</sup>,  
5 Wolfgang Baumgärtner<sup>§</sup>, Jürgen Rehage<sup>†</sup>, Dierck Segelke<sup>§§</sup>, Rosemarie Weikard<sup>\*</sup>, Christa  
6 Kühn<sup>\*,††</sup>

7

8 **Affiliations:**

9 <sup>\*</sup> Leibniz-Institute for Farm Animal Biology (FBN), Institute for Genome Biology, 18196  
10 Dummerstorf, Germany

11 <sup>§</sup> Department of Pathology, University of Veterinary Medicine Hannover, 30559 Hannover,  
12 Germany

13 <sup>†</sup> Clinic for Cattle, University of Veterinary Medicine Hannover, 30173 Hannover, Germany

14 <sup>‡</sup> Department of Small Animal Medicine and Surgery, University of Veterinary Medicine  
15 Hannover, 30559 Hannover, Germany

16 <sup>\*\*</sup> Clinic for Horses, University of Veterinary Medicine Hannover, 30559 Hannover, Germany

17 <sup>§§</sup> Vereinigte Informationssysteme Tierhaltung w.V. (vit), 27283 Verden, Germany

18 <sup>††</sup> Faculty of Agricultural and Environmental Sciences, University Rostock, 18059 Rostock,  
19 Germany

20

21 **Running title:** *T* gene effects on basic mammalian blueprint

22 **Key words:** homeotic transformation, genetic defect, brachyury

23 **Corresponding author:**

24 Christa Kühn

25 Leibniz-Institute for Farm Animal Biology (FBN)

26 Institute for Genome Biology

27 Wilhelm-Stahl-Allee 2, 18196 Dummerstorf, Germany

28 Phone: +49 38208-68709

29 E-mail: [kuehn@fbn-dummerstorf.de](mailto:kuehn@fbn-dummerstorf.de)

30

31

32  
33  
34  
35  
36  
37  
38  
39  
40  
41  
42  
43  
44  
45  
46  
47  
48  
49  
50  
51  
52  
53  
54

## ABSTRACT

A key common feature of all but three known mammalian genera is the strict seven cervical vertebrae blueprint suggesting the involvement of strong conserving selection forces during mammalian radiation. This is further supported by reports indicating that children with cervical ribs die before they reach reproductive age. Hypotheses had been put up associating cervical ribs (homeotic transformations) to embryonal cancer (e.g., neuroblastoma) or ascribing the constraint in cervical vertebral count to the development of the mammalian diaphragm. Here, we describe a spontaneous mutation *c.196A>G* in the *Bos taurus T* gene (also known as *brachyury*) associated with a cervical vertebral homeotic transformation that violates the fundamental mammalian cervical blueprint, but does not preclude reproduction of the affected individual. Genome-wide mapping, haplotype tracking within a large pedigree, resequencing of target genome regions, and bioinformatic analyses unambiguously confirmed the mutant *c.196G* allele as causal for this previously unknown defect termed vertebral and spinal dysplasia (VSD) by providing evidence for the mutation event. The non-synonymous VSD mutation is located within the highly conserved T-box of the *T* gene, which plays a fundamental role in eumetazoan body organization and vertebral development. To our knowledge, VSD is the first unequivocally approved spontaneous mutation decreasing cervical vertebrae number in a large mammal. The spontaneous VSD mutation in the bovine *T* gene is the first *in vivo* evidence for the hypothesis that the T protein is directly involved in the maintenance of the mammalian seven-cervical vertebra blueprint. It therefore furthers our knowledge of the T protein function and early mammalian notochord development.

55

## INTRODUCTION

56 High evolutionary diversification of the vertebral column exists in vertebrates, but the number  
57 of cervical vertebrae within mammals has been fixed at seven for more than 200 million years  
58 of evolution since the beginning of the long and wide mammalian radiation (Hautier *et al.*  
59 2010). The reason why all mammals share this fundamental blueprint of cervical vertebrae,  
60 compared with a more relaxed rule for the number of posterior vertebrae analogous to other  
61 non-mammalian vertebrates, remains unknown. Nevertheless, evolutionary and clinical data  
62 indicate that the cervical vertebral development of mammals is under high selection pressure.  
63 For example, in human pediatrics, 83% of children with a deviating number of cervical  
64 vertebrae die in their first year, while the surviving individuals do not reach reproductive age  
65 (Galis *et al.* 2006). A detailed knowledge of the key factors involved in the spatial regulation  
66 of vertebral development will help to understand these forces.

67 Mutation models, either spontaneous or artificially induced, can reveal the complex processes  
68 that occur during vertebral development. Vertebral and accompanied spinal defects are  
69 described for many species including cattle [e.g., Complex Vertebral Malformation;  
70 (Agerholm *et al.* 2001)] and are often associated with urogenital and intestinal malformations  
71 (van de Ven *et al.* 2011). This association is conclusive due to the coordinated processes of  
72 notochord and cloaca formation during embryonic development. Mutations associated with  
73 spinal and vertebral cord defects are large in number and are located in coding but also in  
74 regulatory regions of many transcription factors (e.g., *Ptf1a* (Vlangos *et al.* 2013)). The  
75 murine *brachyury* (*T*) gene with its mutant alleles was the first gene that was identified and  
76 positionally cloned based on a genetic defect only, the long-known *brachyury* resulting in  
77 vertebral and spinal defects (Dobrovolskaia-Zavadskaia 1927; Herrmann *et al.* 1990).  
78 Numerous subsequent studies confirmed that the coordinated expression of the *T* gene during  
79 gastrulation is essential for appropriate notochord, neural tube, and mesoderm development

80 (Chesley 1935; Pennimpede *et al.* 2012; Satoh *et al.* 2012). Recently, the *T* gene has gained  
81 interest because of its association with the human chordoma, a sporadic and hereditary tumor  
82 originating from relicts of the notochord (Nibu *et al.* 2013; Pillay *et al.* 2012; Yang *et al.*  
83 2009). Thus, the *T* gene is a prime candidate for investigating phenotypic alterations of the  
84 vertebral column and spinal cord.

85 In 2010, early data emerged about newborn calves with short, crooked tails in the Holstein  
86 cattle breed, the most widespread dairy cattle breed worldwide (FAO 2007). For this innate  
87 defect subsequently termed “vertebral and spinal dysplasia” (VSD), initial clinical data had  
88 indicated tail malformations and genealogical analyses a dominant mode of inheritance  
89 (Kromik *et al.* submitted, see Supplemental file). The aim of this study was to provide the  
90 detailed VSD-associated phenotype, to confirm its genetic background and to decipher the  
91 causal mutation for the VSD defect. In our study, we comprehensively i) disclose the  
92 malformations and neurological dysfunctions accompanied with VSD, ii) confirm a genetic  
93 origin and the mode of inheritance for VSD, iii) reveal the causal mutation in the *T* gene and  
94 the founder individual for the defect, and iv) indicate the functional relevance of the mutated  
95 nucleotide. Our study is the first report on a spontaneous mutation inducing a deviation from  
96 the fundamental seven-cervical-vertebrae blueprint in mammals and extends our knowledge  
97 on the functional relevance of the *T* gene regarding neuro-skeletal development.

98

100 **Animals:** The study included registered herdbook individuals with documented ancestry from  
101 the German Holstein dairy cattle population. From an initial on-farm screening for VSD-  
102 affected individuals (Kromik et al. submitted), we selected six calves of different ages and  
103 with different degrees of the congenital VSD associated tail defects (Table S1) for specific,  
104 detailed examinations by specifically trained experts in several specialized units of the  
105 University of Veterinary Medicine Hannover (Germany). This included i) an in-depth  
106 clinical/physical and neurological investigation (including electromyography (EMG) and  
107 motor nerve conduction velocity (mNCV)), ii) a radiological documentation involving X-rays,  
108 and CT and MRI scans with a focus on the spinal cord and vertebral column, iii) a post-  
109 mortem examination and iv) comprehensive laboratory diagnostic analyses of blood,  
110 cerebrospinal fluid (CSF) and serum (Table S2).

111 In addition, sire FBF0666 aging four years at the time of our study was included in  
112 phenotypic analyses, because although he had not shown any signs of a VSD phenotype at  
113 one year of age, but showed increasing locomotion problems with age, analogous to other  
114 reports from farmers of affected calves. For genetic analyses, from the initial on-farm  
115 monitoring (Kromik et al. submitted) individuals from 39 farms were included comprising 85  
116 offspring of the VSD carrier sire FBF0666 (41 classified as VSD affected, 34 classified as  
117 non-VSD affected and 10 with ambiguous VSD classification) and 41 control individuals.  
118 (Table S3). Control calves were all classified as non-VSD affected and matched to target  
119 calves with respect to age, sex, housing conditions, and farm. Furthermore, we included the  
120 dams of the target calves, the carrier sire of the VSD defect (FBF0666), its ancestors and  
121 relatives covering eight generations, as well as 402 randomly selected Holstein and 126  
122 Holstein x Charolais VSD-unaffected calves originating from 110 different sires.

123 **Ethics Statement:** All experimental procedures were carried out according to the German  
124 animal care guidelines and were supervised by the relevant authorities of the States  
125 Mecklenburg-Vorpommern and Niedersachsen, Germany.

126 **Characterization of the VSD Phenotype:** In addition to the standard bovine necropsy  
127 protocol, specific attention was given to those body compartments reported to be associated  
128 with vertebral defects and gait alterations in the literature (including the number and shape of  
129 vertebrae, the skull, peripheral nerves, limb bones, and muscular samples). The complete  
130 vertebral cord was meticulously examined, sampled, and partly macerated for final  
131 documentation.

132 To exclude an effect of epizootic virus diseases that might be involved in the observed  
133 congenital defects, tissue samples were investigated for virus antigens of Bovine virus  
134 diarrhea virus, Bovine herpes virus 1, and Bluetongue virus at the State Laboratory of the  
135 Department of Consumer and Food Safety of Lower-Saxony, Hannover, Germany.

136 For histopathological examination, samples taken during necropsy included the thymus, heart,  
137 lung, pancreas, kidney, bladder, genital apparatus, rumen, abomasum, small and large  
138 intestine, liver, spleen, lymphatic organs, muscles, bones, the central and peripheral nervous  
139 system, and endocrine organs. All samples were examined by light microscopy after  
140 hematoxylin-eosin staining. Furthermore, the spinal cord was investigated by additional  
141 histochemical assays: i) Luxol Fast Blue-Cresyl Echt Violet (myelin), ii) Azan and Masson-  
142 Goldner (collagenous and reticular fibers), and iii) Bielschowsky (neurofilaments).  
143 Additionally, the expression pattern of selected antigens was monitored by  
144 immunohistochemistry including i) glial fibrillary acidic protein (GFAP), ii) myelin basic  
145 protein (MBP), iii) amyloid precursor protein (APP), iv) factor VII related antigen, and v)  
146 vimentin. Histochemistry and immunohistochemistry were performed according to Ulrich and  
147 colleagues (Ulrich *et al.* 2010) .

148 **Karyotyping:** The karyotypes of the carrier sire and one severely affected offspring were  
149 investigated to identify chromosomal aneuploidy or translocation. Blood samples were taken  
150 and metaphase chromosomes were prepared according to standard procedures (Popescu *et al.*  
151 2000). Chromosome morphology was visualized after Giemsa staining by light microscopy.

152 **Genetic Mapping of the VSD Locus:** For genotyping, blood/sperm samples from sire  
153 FBF0666, its dam FBF0266, its sire FBF0667, maternal grandsire FBF0669 and from all 126  
154 calves included in the clinical and epidemiological survey and 73 dams were included. All  
155 DNA samples were genotyped with the BovineSNP50 v2 BeadChip (Illumina, San Diego,  
156 CA, USA) and analyzed using Genome Studio (Illumina, San Diego, CA, USA) software.  
157 SNPs were filtered for call frequency  $>0.97$ . All SNPs with heterozygote excess (deviation  
158 from Hardy-Weinberg equilibrium identified by  $p(\chi^2_{HWE}) < 0.05$ ), gene train score  $< 0.6$ , or  
159 minor allele frequency  $< 0.01$  were manually checked. Only those samples with a call rate  
160  $> 0.98$  without pedigree conflicts were included in subsequent analyses.

161 Initial twopoint linkage mapping between each of the SNPs and the VSD locus was  
162 performed in the half-sibship originating from sire FBF0666. An autosomal dominant  
163 inheritance was assumed as indicated by the initial epidemiological analysis (Kromik *et al.*,  
164 submitted) and an equal distribution of VSD cases across both sexes in the FBF0666 sibship.  
165 Consequently, the VSD locus was coded as heterozygous “1/2” in sire FBF0666 and all  
166 affected offspring, whereas all dams (assumed to be non-affected) and non-affected offspring  
167 were coded as homozygous “1/1”. Mapping was carried out along the entire autosomal  
168 genome (BTA1 to BTA29) with the TWOPOINT option of CRIMAP version 2.50 (Green *et*  
169 *al.* 1990) incorporating modifications by Ian Evans and Jill Maddox (University of  
170 Melbourne, Australia).

171 After obtaining a strong indication of the genomic position of the VSD locus on BTA9, a  
172 multipoint mapping approach was conducted using MERLIN version 1.1.2 (Abecasis *et al.*



173 2002) with the affected code assigned to all VSD-affected offspring and sire FBF0666, and  
174 the non-affected status assigned to all dams and those offspring categorized as non-affected.  
175 For this purpose, a BTA9 marker map required for multipoint mapping was established with  
176 CRIMAP CHROMPIC options from the genotypes in the half-sib family. Markers with  
177 identical genetic positions were artificially separated by 0.001 cM to enable the running of the  
178 multipoint algorithm implemented in MERLIN. To account for potential incomplete  
179 penetrance of the defect, a 0.2, 0.6, and 1.0 penetrance of an autosomal dominant defect was  
180 modeled.

181 **Haplotyping:** All available offspring of sire FBF0666 were haplotyped for BTA9 using  
182 CRIMAP CHROMPIC options. After extracting the paternally inherited haplotype of each  
183 FBF0666 offspring, these haplotypes were aligned to identify the chromosomal segment  
184 shared by all VSD-affected individuals. All physical positions of SNPs and haplotype borders  
185 were indicated according to the bovine genome assembly UMD3.1 (Zimin *et al.* 2009).

186 To further trace the origin of the haplotype associated with VSD, we subsequently haplotyped  
187 all available dams and the FBF0666 ancestors in the German Holstein population using  
188 BEAGLE (Browning & Browning 2009). Haplotyping included a total of 55,384 individuals  
189 from the Holstein population with BovineSNP50Illumina SNP-Chip genotype information  
190 provided by VIT Verden (<http://www.vit.de/index.php?id=milchrinder-zws-online&L=1>), the  
191 central database for genomic evaluation in German Holstein cattle.

192 **Resequencing of the Candidate Locus:** The *T* gene was resequenced for a potentially causal  
193 mutation in VSD-affected and non-affected calves, in sire FBF0666, in the parents of sire  
194 FBF0666, and also in the maternal grandsire of sire FBF0666. All primers used for  
195 sequencing the *T* gene are indicated in Table S4. The obtained sequences were aligned to the  
196 mRNA reference sequence ([http://www.ncbi.nlm.nih.gov/nuccore/NM\\_001192985](http://www.ncbi.nlm.nih.gov/nuccore/NM_001192985)) and the  
197 respective genomic sequence ([http://www.ncbi.nlm.nih.gov/nuccore/AC\\_000166.1](http://www.ncbi.nlm.nih.gov/nuccore/AC_000166.1)).

198 **Population Screening for the Causal Mutation:** We genotyped 94 sons of FBF0669, the  
199 sire FBF0666's maternal grandsire, at the *T c.196A>G* polymorphism to further confirm its  
200 causal characteristics and to validate the founder individual of the VSD mutation. All 94  
201 offspring were sires themselves with at least 200 offspring each and with no report suggesting  
202 VSD cases in the first-generation descendants of these bulls. In addition, 39 of the VSD-  
203 unaffected control calves, 402 randomly selected purebred Holstein and 126 Holstein x  
204 Charolais crossbred calves were genotyped. All calves had shown no indication of VSD upon  
205 physical examination. For genotyping, a KASP assay addressing the mutation *T c.196A>G*  
206 was developed (LGC Genomics, KBioscience, Hoddesdon, UK). Genotyping was performed in  
207 a 10 µl reaction solution using 20 ng DNA on a Lightcycler 480 (Roche Applied Science,  
208 Mannheim, Germany) according to the manufacturer's recommendation for KASP assays but  
209 with the exception of an increase in MgCl<sub>2</sub> concentration by 0.3 mM (for primers see Table  
210 S4).

211 **Bioinformatic Analyses:** The wild-type and mutated (VSD) amino acid sequences of the  
212 bovine T protein were submitted for 3D protein structure prediction using Phyre2  
213 ([http://www.sbg.bio.ic.ac.uk/~phyre2/html/](http://www.sbg.bio.ic.ac.uk/~phyre2/html/page.cgi?id=index) page.cgi?id=index, (Kelley & Sternberg 2009)).  
214 To further predict the functional effects of the non-synonymous c.196A>G transition, wild-  
215 type and mutated (VSD) amino acid sequences of the bovine brachyury T were also submitted  
216 to Polyphen2 analysis (<http://genetics.bwh.harvard.edu/pph2/>, (Adzhubei *et al.* 2010)).  
217 Analysis of sequence homology across species was performed by Homologene  
218 (<http://www.ncbi.nlm.nih.gov/homologene>).

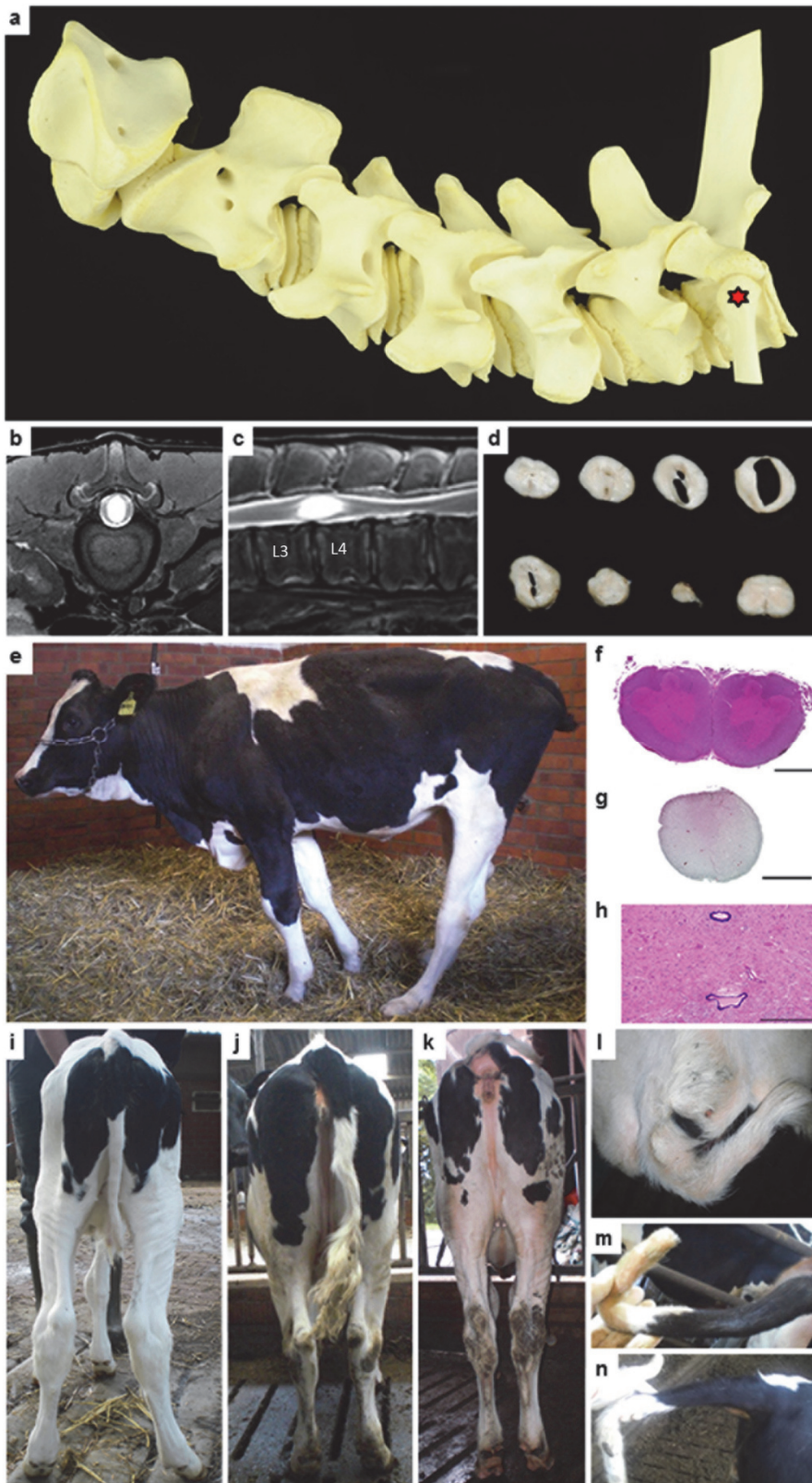
219

220

## RESULTS

### 221 **VSD is Characterized by a Variable Number of Vertebrae and Neurological Deficits**

222 Radiological examination (X-ray, computed tomography (CT) and magnetic resonance  
223 imaging (MRI)) and necropsy of calves with divergent degrees of clinical VSD-associated tail  
224 malformations confirmed that the calves shared vertebral defects, including dysplasia and  
225 numerical aberrations in all parts of the spine except the sacrum (Table S1). The most striking  
226 feature was the cervical homeotic transformation (Figure 1) resulting in reduction of the  
227 cervical vertebrae number in four of the six necropsied calves. In addition to malformations of  
228 the vertebral column, variably expressed defects of the spinal cord restricted to the  
229 lumbosacral segment were found including syringomyelia (mostly accompanied with  
230 hydromyelia), diplomyelia, a duplicated central canal, and segmental hypoplasia (Figure 1,  
231 Figure S1, Table S1). The double central channel and the diplomyelia were exclusively  
232 observed in the sacral segment of the spinal cord and suggest a duplication event during  
233 neural development. Histochemistry and immunohistochemistry showed that in calves with  
234 prominent syringomyelia/hydromyelia a reduced number of axons in the lumbar white matter  
235 were detected that might be interpreted as hypoplasia. Furthermore, reactive astrogliosis was



236

237 **Figure 1.** Clinical, Radiological, Pathological and Histological Features of the VSD Phenotype in Affected  
 238 Calves

239 [a] Macerated cervical vertebral column of a calf affected by VSD showing homeotic thoracic transformation of  
 240 the seventh cervical vertebra (see red asterisk: the seventh vertebra articulating with the tuberculum costae of the  
 241 first rib. [b, c] Transversal (b) and sagittal (c) MRI scans of a one day old calf with severe non-ambulatory  
 242 paraparesis: prominent hyperintense fluid-filled central canal cavity (syringo-hydromyelia) in the lumbar spinal  
 243 cord at the segment L1 to L2 and a massively reduced transverse diameter of the spinal cord at L3 and L4. [d]

244 Stepwise transverse sections of the lumbar spinal cord segments L1 to L4 (shown in b, c) displaying  
245 communicating hydromyelia and syringomyelia followed by segmental dysplasia and hypoplasia. [e] Calf with  
246 VSD phenotype showing a non-physiological forward positioning of the hind legs with straightened hocks. [f]  
247 Diplomyelia of the sacral segment of the spinal cord, scale bar 25 mm. [g] Hypo- and dysplasia of the middle  
248 lumbar segment of the spinal cord including missing ventral median fissure, scale bar 25 mm. [h] Duplication of  
249 the central canal in the sacral segment of the spinal cord, scale bar 500  $\mu\text{m}$ . [i] Seven day old calf with slightly  
250 shortened and kinked tail defect combined with slightly hyperextended flexor tendons and external rotation of  
251 the hind limbs (left < right). [j] Seven months old calf with distinct kinked tail defect and slight rotation of the  
252 hind limbs (left < right). [k, l] Rear and dorsal view of an eight month old calf with a severe crooked tail defect  
253 and external rotation of the hind limbs. [m - n] Separation in coccygeal vertebral column as a part of a tail defect.  
254

255 detected, shown as a small zone with strong accumulated GFAP positive cell dendrites around  
256 the syringomyelia. Further immunohistochemistry analyses of the spinal cord did not reveal  
257 additional abnormalities. All other tested neuroproteins were expressed regularly. Results  
258 from the neurological investigation matched the impaired posterior spinal structures and  
259 revealed multiple functional deficits associated with VSD. Specifically, VSD-affected calves  
260 displayed spasticity, paraparesis, impaired spinal reflexes, and ataxia which were  
261 predominantly expressed in the hind limbs (Table S5, File S1). However, VSD was not  
262 associated with intestinal, urogenital, cerebral, or skull defects in contrast to many other  
263 mammalian vertebral malformation defects (Vlangos *et al.* 2013). Biochemical and  
264 hematological tests monitoring enzyme activities, metabolites, electrolytes in serum as well as  
265 protein value and blood cell count in cerebrospinal fluid did not reveal any significantly  
266 increased incidence of deviation from norm values in VSD-affected calves. Furthermore,  
267 there was no evidence of Bovine Herpes Virus 1, Bluetongue or Bovine Virus Diarrhea virus  
268 in any of the necropsied, affected VSD calves.

269

## 270 **VSD is an Autosomal Dominantly Inherited Defect with Incomplete Penetrance**

271 VSD cases showed substantial variation regarding the degree of physical and neurological  
272 alterations associated with the defect (severe cases with non-ambulatory paraparesis to mild  
273 cases displaying only minor tail defects, Tables S1 and S5). The hypothesis of a dominant  
274 VSD allele effect previously indicated by an almost equal proportion of VSD affected and

275 non-affected offspring of sire FBF0666 is further supported by sire FBF0666, which itself  
276 clearly expressed the VSD phenotype as determined by pathological examination (Table S1).

277

## 278 **VSD is Localized on Bovine Chromosome 9**

279 Initial karyotyping of sire FBF0666 and a severely affected offspring did not reveal any  
280 numerical abnormalities or large structural chromosomal aberrations. The equal distribution  
281 of VSD cases across both sexes in the FBF0666 sibship (Table S1) indicated an autosomal  
282 localization of the defect. The Crooked Tail Syndrome (CTS), a well-described bovine defect  
283 affecting tail morphology (Fasquelle *et al.* 2009), had been excluded as causal background for  
284 VSD due to a homozygous wild type genotype of sire FBF0666 at the causal mutation locus  
285 for CTS (Kromik *et al.* submitted).

286 A whole-genome scan in the *Bos taurus* genome yielded SNPs on two chromosomes with  
287 Logarithm of the Odds (LOD) scores  $> 3$  for linkage to VSD: 99 SNPs on bovine  
288 chromosome (BTA) 9 and a single SNP on BTA17 (Figure 2, Table S6). On BTA9,  
289 exclusively SNPs located between 85,175,167 bp (rs41604518) and 105,074,182 bp  
290 (rs41619164) showed a significant LOD score  $> 3.0$  in the twopoint analyses. The subsequent  
291 multipoint test statistic obtained by parametric linkage analysis placed the VSD locus in a  
292 LOD drop 3 confidence interval between rs110768165 (102,711,446 bp) and rs109233157  
293 (104,196,469 bp). Alignment (Figure 2, Figure S2) of the paternally inherited BTA9  
294 haplotypes of all FBF0666 offspring with VSD phenotype showed that all these individuals  
295 shared a common haplotype spanning from rs110492820 (100,138,190 bp) to rs109532989  
296 (102,851,852 bp). This narrowed down the target interval for the VSD mutation to 2.7 Mb in  
297 the telomeric region of BTA9.

298



300 **Figure 2.** Mapping and Identification of the VSD Mutant Allele  
301 [a] Manhattan plot showing the results (LOD scores) of the genome-wide twopoint linkage analysis between all  
302 tested SNPs and the VSD locus. LOD score threshold 3.0 is indicated by the red horizontal line. [b] LOD scores  
303 from twopoint linkage analysis (blue dots) and multipoint linkage analysis (green line) on BTA9. The light  
304 yellow box shows the LOD drop 3 confidence interval in the telomeric region on BTA9. ‘x’ and ‘o’ denote  
305 alternative paternal alleles inherited by the respective offspring, ‘-’ indicates non-informative allele regarding  
306 paternal origin. [c] Selection of aligned paternally inherited BTA9 haplotypes (for all data see Figure S2) in the  
307 telomeric region of BTA9. The VSD-affected offspring of sire FBF0666 shared a common haplotype (HT2)  
308 spanning from rs110492820 (100,138,190 bp) to rs109532989 (102,851,852 bp). The phenotypically unaffected  
309 offspring of sire FBF0666 showed the alternative paternal haplotype (HT1) (black) except two individuals that  
310 had inherited the VSD-associated haplotype (red-boxed black). Yellow boxes indicate recombination events that  
311 set the limits of the VSD haplotype. [d] All annotated genes (Ensembl annotation release 75) in the chromosomal  
312 region 100-103 Mb including the prime candidate bovine *T* gene (light yellow box).  
313 [e] Exon-intron structure of the bovine *T* gene according to Refseq sequence NM\_001192985.1. Exon 1  
314 containing the mutation causal for VSD is indicated in red. [f] Electropherogram showing a part of the exon 1  
315 nucleotide sequence of the bovine *T* gene in a VSD-unaffected calf with the wild type genotype A/A at position  
316 c.196 and in a VSD-affected calf with the heterozygous genotype A/G at position c.196. [g] Domain composition  
317 of the bovine T protein with position 66 of the amino acid sequence affected by the polymorphism c.196A>G  
318 causal for VSD. The T-box is indicated as well as both transcription activation domains (TA1 and TA2) and both  
319 repression domains (R1 and R2). Domain annotation according to NCBI Conserved Domain Database (CDD)  
320 ([http://www.ncbi.nlm.nih.gov/Structure/cdd/wrpsb.cgi?seqinput=NP\\_001179914.1](http://www.ncbi.nlm.nih.gov/Structure/cdd/wrpsb.cgi?seqinput=NP_001179914.1)) and (Satoh *et al.* 2012).  
321

## 322 **Tracing the Haplotype Associated with VSD in the Affected Pedigree**

323 Haplotype tracking in an eight generation pedigree clearly demonstrated that sire FBF0666  
324 had inherited the VSD-associated haplotype (position 100,138,190–102,851,852 bp) from its  
325 dam (FBF0266, Figure 3, Figure S3). Further tracing back of the inheritance of this haplotype  
326 showed that the dam had been inbred to its sire (FBF0669) and carried identical by state (IBS)  
327 chromosomal segments to both sire FBF0669’s haplotypes in the VSD target region.  
328 However, analysis of the haplotypes for the entire BTA9 revealed that sire FBF0669 had  
329 forwarded to FBF0266 the respective haplotype (position 100,138,190–102,851,852 bp),  
330 which was shared by all VSD affected FBF0666 offspring (Figure S3, red haplotypes). The  
331 alternative haplotype of sire FBF0669 (Figure S3, blue haplotypes; Figure 3) was obviously  
332 not associated with VSD. This is supported by population data: In our eight generation  
333 pedigree, no previous reports on VSD-like defects were obtained in the first-generation  
334 offspring of confirmed carriers of the alternative non-VSD FBF0669 haplotype (sires  
335 FBF0670, FBF0671, FBF0672, and FBF0673; Figure 3), although these bulls had sired  
336 several hundred thousand offspring worldwide.



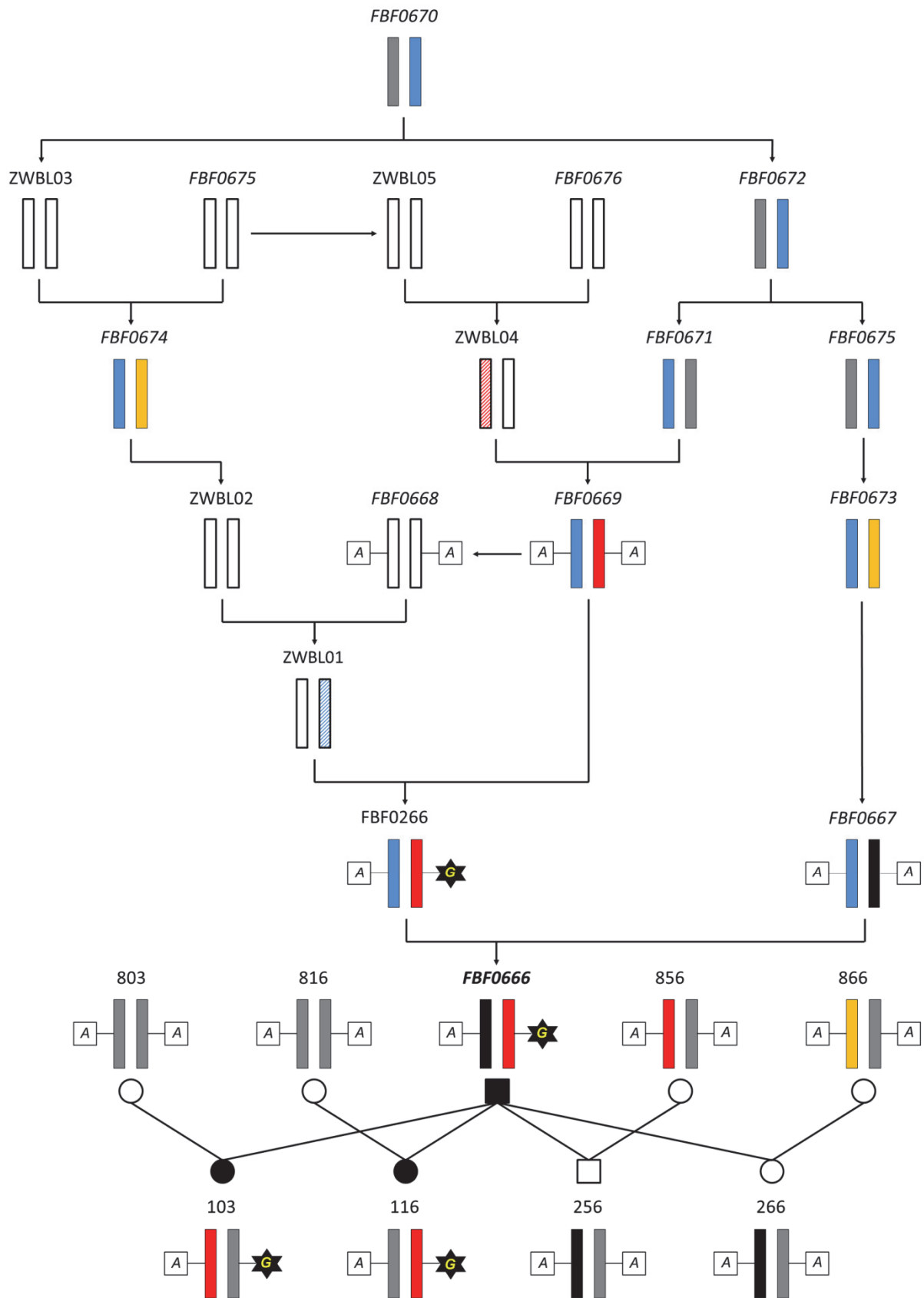
337

338 **VSD Is Caused by a *de-novo* Mutation in the T Gene**

339 In the current bovine genome assemblies, the target interval for the causal mutation (BTA9:  
340 100,138,190–102,851,852 bp) harbors 23 annotated or putative genes (Figure 2, NCBI  
341 annotation release 103: accession date 2014/03/18, [http://www.ncbi.nlm.nih.gov/projects/  
342 mapview/map\\_search.cgi?taxid=9913&build=103.0](http://www.ncbi.nlm.nih.gov/projects/mapview/map_search.cgi?taxid=9913&build=103.0); Ensembl: [http://www.ensembl.org  
343 /Bos\\_taurus/Location/View?g=ENSBTAG00000018681;r=9:102662033-102680686;  
344 t=ENSBTAT00000024865](http://www.ensembl.org/Bos_taurus/Location/View?g=ENSBTAG00000018681;r=9:102662033-102680686;t=ENSBTAT00000024865), accession date 2014/03/18). Of these, the *T* gene stood out as the  
345 single prime functional candidate gene responsible for the vertebral and spinal malformations  
346 of VSD because of the previously reported effects of *T* gene mutations on embryonic  
347 notochord development and on tail length (Haworth *et al.* 2001; Herrmann *et al.* 1990).  
348 Resequencing of the *T* locus in cow FBF0266, in sires FBF0666, FBF0667, FBF0669, in  
349 VSD-affected and non-affected FBF0666 offspring as well as in unrelated individuals  
350 revealed an A>G transition polymorphism at position c.196 of the *T* gene (according to  
351 NM\_001192985.1, Figure 2). This non-synonymous mutation is located in exon 1 of the *T*  
352 gene (according to NM\_001192985.1) and results in a substitution of the amino acid lysine by  
353 glutamic acid at position 66 of the T protein sequence (p.66Lys>Glu). Only sire FBF0666,  
354 VSD-affected calves, five calves phenotypically unaffected but carrying the VSD-associated  
355 haplotype (e.g., FBF249 and FBF250, Figure 2) and dam FBF0266 carried the mutated allele  
356 (Figure 3). The observation of *T c.196G* carriers without clinical phenotype underlines the  
357 hypothesis of incomplete penetrance for VSD. However, sire FBF0669, from which cow  
358 FBF0266 had inherited the VSD-associated haplotype, was homozygous for the wild-type  
359 nucleotide at position c.196 (Figure 3).

360

361



362

363  
364  
365  
366

**Figure 3.** Tracing the VSD-associated Haplotype and the Origin of the VSD Mutation  
Haplotypes in the target area of BTA9 (100,138,190 bp to 102,851,852 bp) are indicated by long rectangles within an eight generation Holstein pedigree segregating for the VSD. Red rectangle: maternally inherited haplotype of sire FBF0666; black rectangle: alternative haplotype of sire FBF0666; blue: non-VSD-associated

367 haplotype in the dam FBF0266 of sire FBF0666; fawn: haplotype identical by state to the VSD-associated sire  
368 FBF0666 haplotype except for the SNP rs29023535 (102,690,968 bp) at the telomeric end; grey: further  
369 haplotypes. Striped colored haplotypes were concluded from the haplotypes of the offspring according to  
370 Mendelian rules of inheritance; blank haplotypes are unknown. VSD-affected animals according to clinical,  
371 neurological and/or pathological examination are indicated by black boxes/circles. Individuals with confirmed  
372 non-affected phenotype are indicated by open boxes/circles. For confirmation of inherited haplotypes for dam  
373 FBF0266 see Figure S3. Letters in boxes or stars, respectively, indicate haplotype-associated alleles at position  
374 c.196A>G in the bovine *T* gene determined by sequencing.

375

376 Although sire FBF0669 has more than 140,000 registered daughters born in two decades,  
377 there are no reports of VSD within this large sibship suggesting that it is extremely unlikely  
378 that the sire carries the dominant causal VSD mutation. The homozygous wild-type genotype  
379 of 94 male offspring from sire FBF0669, as determined by genotyping of the VSD locus *T*  
380 *c.196A>G*, also supported the homozygous wild-type status of sire FBF0669 at this  
381 chromosomal position. These 94 offspring are themselves widely-used sires with at least 200  
382 offspring born to each. The absence of VSD incidence reports in the first-generation  
383 descendants of these 94 bulls corresponds to their wild-type genotype at the VSD locus.

384 Thus, haplotype tracking and mutation analysis clearly demonstrate that *T c.196A>G* is a *de*  
385 *novo* mutation in cow FBF0266 not previously seen on the respective haplotype.  
386 Consequently, only the direct progeny of cow FBF0266 could possibly carry the mutated  
387 allele associated with VSD. Indeed, genotyping of 39 VSD-unaffected control calves  
388 (matched controls to FBF0666 offspring) and a further 528 randomly selected Holstein and  
389 Holstein x Charolais calves did not identify any carrier of the mutant *T c.196G* allele. In  
390 addition, seven VSD unaffected calves' dams in our dataset, which are no direct offspring to  
391 dam FBF0266, but which carried the VSD haplotype in a IBS homo- or heterozygous state  
392 (determined according to 50k SNP haplotyping), were all homozygous for the wild-type allele  
393 *T c.196A*.

394

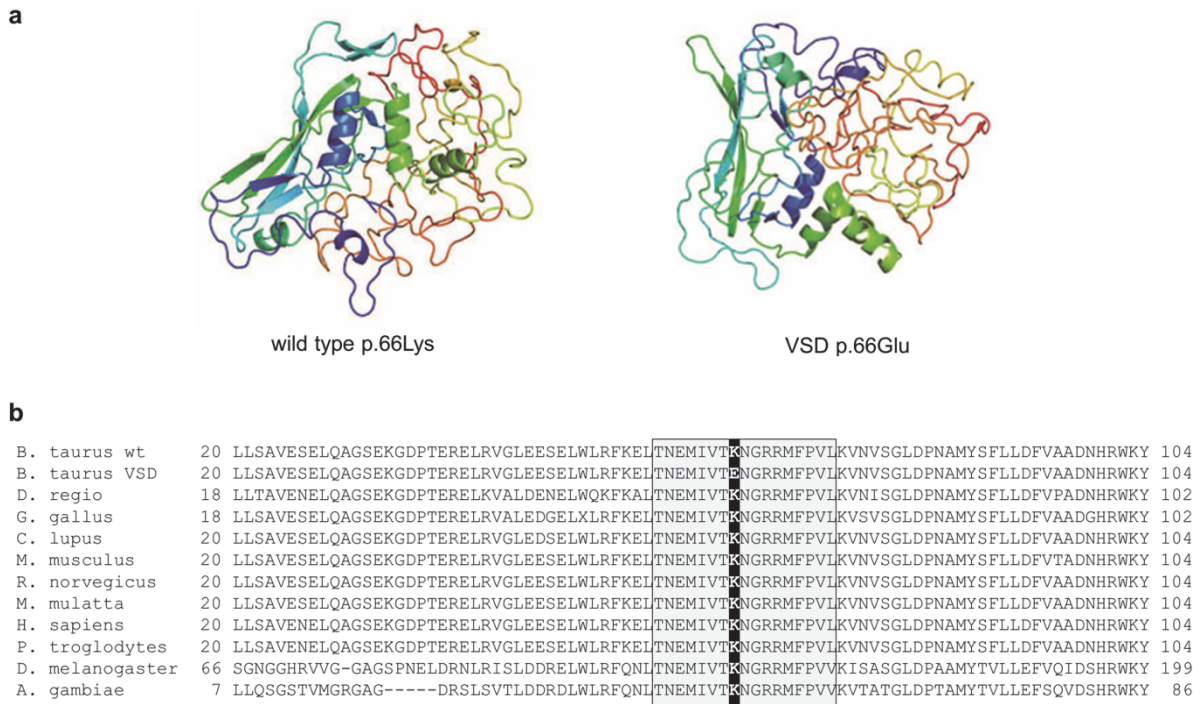
## DISCUSSION

395

396 Our study is the first report of the inherited *Bos taurus* defect VSD that is associated with a  
397 reduced number of cervical vertebrae, a unique, striking feature that had not yet been  
398 described for a spontaneous mutation in any mammalian species before. The *T* gene belongs  
399 to the family of T-box genes that encode transcription factors consisting of transcriptional  
400 activator and/or repressor domains and a DNA binding T-box domain in many eukaryotic  
401 species including vertebrates and invertebrates (Sato *et al.* 2012). The T protein is essential  
402 for development of the notochord and mesoderm formation in the primitive streak during  
403 early embryonic vertebrate development (Kispert & Herrmann 1994). Experimental  
404 crystallographic data for the T protein (Müller & Herrmann 1997) demonstrated that the  
405 amino acid position equivalent to the variant amino acid position p.66Lys>Glu in the bovine  
406 ortholog is located at a critical site in the DNA binding T-box domain of the T protein (Figure  
407 2). Specifically, the amino acid position p.66 forms polar interactions with the DNA target  
408 and is directly involved in the DNA binding of the T-box domain and dimerization of the T  
409 protein during DNA binding. It is conclusive that replacing the wild-type basic amino acid  
410 lysine by the mutant acidic amino acid glutamic acid at p.66 in the bovine T protein will  
411 substantially disturb those T protein binding properties. This is supported by bioinformatic  
412 analyses predicting considerable changes in the three-dimensional peptide conformation of  
413 the bovine T protein as a result of the missense mutation (Figure 4) and also by estimating  
414 mutation effects (“probably damaging” score: 0.977, according to Polyphen2 (Adzhubei *et al.*  
415 2010). Finally, HomoloGene analysis showed that the position homologous to bovine T p.66  
416 is highly conserved from *Homo sapiens* down to *Drosophila melanogaster* and *Anopheles*  
417 *gambiae* (Figure 4). This strong conservation further confirms a fundamental relevance of the  
418 protein, particularly at the position affected by the mutation. Because classical gene rescue  
419 experiments to prove causality of a mutation are extremely difficult in cattle, we further  
420 followed the guidelines for investigating causality of sequence variants in human disease

421 (MacArthur *et al.* 2014). In this line, the conclusion of a causal role for the *T c.196A>G*  
422 mutation in VSD is further supported by comparative data. Already Chesley (Chesley 1935)  
423 reported that mice heterozygous for a mutant T allele showed effects on the notochord at the  
424 early stage of development (day 8) and also on the neural tube. Mutations in several parts of  
425 the *T* gene often show a similar mode of inheritance and a variable penetrance (e.g., the Manx  
426 syndrome in cats (Buckingham *et al.* 2013)). Furthermore, the mutations in the *T* gene are  
427 associated with tail defects or malformation of posterior parts of the body in many other  
428 species from drosophila to mice, cats and dogs (Buckingham *et al.* 2013; Haworth *et al.* 2001;  
429 Herrmann *et al.* 1990; Kispert *et al.* 1994; Odenthal *et al.* 1996). In human, a recessively  
430 acting mutation in the *T* gene has been identified to be associated with fusion of cervical  
431 vertebrae, with sacral agenesis and/or abnormal notochord features (Ghebranious *et al.* 2008;  
432 Postma *et al.* 2014). Furthermore, for the mouse *T* curtailed (*T<sup>c</sup>*) allele there is one study  
433 reporting effects on the cervical vertebrae (Searle 1966), whereas *T* gene mutant alleles  
434 mostly affected the posterior part of the vertebral column. However, the specific effects  
435 observed in murine *T<sup>c</sup>* heterozygotes and human patients heterozygous for the *T c.1013C>T*  
436 mutation are different to those of VSD heterozygotes, because there is no lack, but a fusion of  
437 two or more vertebrae. Also in contrast to *T<sup>c</sup>*, in the VSD-affected animals the sacrum is the  
438 only part of the bony vertebral column without malformation. To our knowledge, none of the  
439 known *T* mutations in other species showed effects of cervical vertebral deletions/homeotic  
440 transformations, not even for homozygous individuals. In *Bos taurus*, other lethal genetic  
441 defects associated with vertebral malformations (Complex cervical malformation,  
442 Brachyspina) could be excluded as background for the VSD defect, because both defects had  
443 been localized on BTA3 or BTA21, respectively (Charlier *et al.* 2012; Thomsen *et al.* 2006).  
444 Our results suggest that the VSD mutation affects the primitive streak as well as the tail bud  
445 because vertebrae originating from both precursors are affected by the mutation: cervical  
446 vertebrae originating from the primitive streak and coccygeal vertebra originating from the

447 tail bud. This fits the observation that murine *T* +/- heterozygous embryos showed a 50%  
 448 reduction of *T* gene expression in the tail bud and notochord compared with wild-type mice  
 449 (Pennimpe *et al.* 2012).



450

451 **Figure 4.** Predicted Conformation Change of the Wild-Type and VSD Bovine T Protein and T Protein  
 452 Interspecies Amino Acid Sequence Comparison

453 [a] Predicted 3D-structure of the wild-type (p.66Lys) and mutated (VSD, p.66Glu) bovine T protein as  
 454 determined by the bioinformatic prediction tool Phyre2 ([http://www.sbg.bio.ic.ac.uk/~phyre2/html/](http://www.sbg.bio.ic.ac.uk/~phyre2/html/page.cgi?id=index)  
 455 [page.cgi?id=index](http://www.sbg.bio.ic.ac.uk/~phyre2/html/page.cgi?id=index)).

456 [b] HomoloGene (<http://www.ncbi.nlm.nih.gov/homologene>) analysis of the T protein/homologue encompassing  
 457 the variant bovine amino acid position 66 (indicated by black background) across vertebrates and insects (*Danio*  
 458 *regio*: [XP\\_001343633.3](#), *Gallus gallus* [NP\\_990271.1](#), *Bos taurus* [NP\\_001179914.1](#), *Canis lupus*  
 459 [NP\\_001003092.1](#), *Mus musculus* [NP\\_033335.1](#), *Rattus norvegicus* [NP\\_001099679.1](#), *Macaca mulatta*  
 460 [XP\\_001101514.1](#), *Homo sapiens* [NP\\_003172.1](#), *Pan troglodytes* [XP\\_527563.3](#), *Drosophila melanogaster*  
 461 [NP\\_524031.2](#), *Anopheles gambiae* [XP\\_320606.4](#)). Boxed and marked with gray background is the longest fully  
 462 conserved segment within the entire T protein/homologue. wt: wild-type allele, VSD: VSD-associated allele.

463

464 Pennimpe and colleagues (Pennimpe *et al.* 2012) previously suggested that the T protein  
 465 is directly involved in the maintenance of the mammalian seven-cervical vertebra blueprint  
 466 because of the homeotic C7 > T1 transformation of cervical vertebrae in 30% of mice from *in*  
 467 *vivo* *T* gene knockdown experiments. The spontaneous VSD mutation in the bovine *T* gene is  
 468 the first *in vivo* evidence for this hypothesis from a mutation model. Our data also highlight a  
 469 distinct amino acid position (p.66) that might be relevant for a coordinated Wnt–brachyury–

470 HOX signaling cascade, which is important for cervical vertebral and spinal cord  
471 development (Galis 1999; Yamaguchi *et al.* 1999). Remarkably, the heterozygous VSD  
472 genotype causes substantial phenotypic impairments, whereas even murine *T* null-alleles, in  
473 which the *T* locus is completely absent, only cause mild phenotypic defects in heterozygotes  
474 (Smith 1997). This expression pattern of the VSD phenotype suggests a dominant negative  
475 effect of the VSD allele. A similar mechanism was also suggested for some alleles at the  
476 murine *brachyury* locus ( $T^c$ ,  $T^{wis}$ ), although these alleles alter the carboxy-terminus of the T  
477 protein (Herrmann & Kispert 1994), which potentially acts as activating domain and in  
478 contrast to the T-box domain shares little sequence similarity between species (Smith 1997).  
479 Although there are many similarities of the VSD mutation to tail defects in other species, to  
480 our knowledge no other spontaneous mutation in the *T* gene or other mammalian genes causes  
481 a homeotic transformation of cervical vertebrae similar to VSD. In addition, VSD is also  
482 unique, because in spite of congenital homeotic transformation of cervical vertebrae, affected  
483 individuals survive to reproductive age and show no primary defects outside vertebral spine  
484 and spinal cord.

485

486

#### ACKNOWLEDGEMENTS

487 The project was funded by the Förderverein Biotechnologieforschung (FBF), Bonn, Germany.  
488 We thank Jill Maddox (University of Melbourne, Australia) for providing the modified  
489 CRIMAP Version 2.50. We are indebted to the Masterrind GmbH, Verden and its associated  
490 farmers for bringing the congenital effect to knowledge and assisting in data collection.  
491 Specifically, Dr. D. Frese and Dr. H. Osmers contributed valuable input during fruitful  
492 discussions. Technical assistance of Simone Wöhl, Antje Lehmann and Marlies Fuchs is  
493 thankfully acknowledged. Important help was provided by colleagues in the animal  
494 experimental units of the Leibniz Institute for Farm Animal Biology (FBN).

495

## LITERATURE CITED

496 Abecasis, G. R., S. S. Cherny, W. O. Cookson, and L. R. Cardon, 2002 Merlin-rapid analysis  
497 of dense genetic maps using sparse gene flow trees. *Nat. Genet.* **30**: 97-101.

498 Adzhubei, I. A., S. Schmidt, L. Peshkin, V. E. Ramensky, A. Gerasimova *et al.* 2010 A  
499 method and server for predicting damaging missense mutations. *Nat. Meth.* **7**: 248-  
500 249.

501 Agerholm, J. S., C. Bendixen, O. Andersen, and J. Arnbjerg, 2001 Complex vertebral  
502 malformation in Holstein calves. *J. Vet. Diagn. Invest.* **13**: 283-289.

503 Browning, B. L., and S. R. Browning, 2009 A unified approach to genotype imputation and  
504 haplotype-phase inference for large data sets of trios and unrelated individuals. *Am. J.*  
505 *Hum. Genet.* **84**: 210-223.

506 Buckingham, K. J., M. J. McMillin, M. M. Brassil, K. M. Shively, K. M. Magnaye *et al.*  
507 2013 Multiple mutant T alleles cause haploinsufficiency of Brachyury and short tails  
508 in Manx cats. *Mamm. Genome* **24**: 400-408.

509 Charlier, C., J. S. Agerholm, W. Coppieters, P. Karlskov-Mortensen, W. Li *et al.* 2012 A  
510 Deletion in the Bovine FANCI Gene Compromises Fertility by Causing Fetal Death  
511 and Brachyspina. *Plos One* **7**: e43085.

512 Chesley, P., 1935 Development of the short-tailed mutant in the house mouse. *J. Exp. Zool.*  
513 **70**: 429-459.

514 Dobrovolskaia-Zavadskaia, N., 1927 Sur la mortification spontanee de la queue chez la souris  
515 nouveau-nee et sur l'existence d'un caractere hereditaire <<non viable>>. *CR Soc Biol*  
516 **97**: 114-116.



517 FAO, 2007 *The state of the World's Animal Genetic Resources for Food and Agriculture*.  
518 Rome, Italy.

519 Fasquelle, C., A. Sartelet, W. B. Li, M. Dive, N. Tamma *et al.* 2009 Balancing Selection of a  
520 Frame-Shift Mutation in the MRC2 Gene Accounts for the Outbreak of the Crooked  
521 Tail Syndrome in Belgian Blue Cattle. *Plos Genet.* **5**: e1000666.

522 Galis, F., 1999 Why do almost all mammals have seven cervical vertebrae? Developmental  
523 constraints, Hox genes, and cancer. *J. Exp. Zool.* **285**: 19-26.

524 Galis, F., T. J. Van Dooren, J. D. Feuth, J. A. Metz, A. Witkam *et al.* 2006 Extreme selection  
525 in humans against homeotic transformations of cervical vertebrae. *Evolution* **60**: 2643-  
526 2654.

527 Ghebraniou, N., R. D. Blank, C. L. Raggio, J. Staubli, E. Mcpherson *et al.* 2008 A Missense  
528 T(Brachyury) Mutation Contributes to Vertebral Malformations. *J. Bone Miner. Res.*  
529 **23**: 1576-1583.

530 Green, P., K. Falls, and S. Crooks, 1990 Documentation of CRI-MAP version 2.4.  
531 Unpublished mimeo (<http://www.animalgenome.org/hu/CRIMAPwkshp/crimap-doc.html>).  
532

533 Hautier, L., V. Weisbecker, M. R. Sanchez-Villagra, A. Goswami, and R. J. Asher, 2010  
534 Skeletal development in sloths and the evolution of mammalian vertebral patterning.  
535 *Proc. Natl. Acad. Sci.* **107**: 18903-18908.

536 Haworth, K., W. Putt, B. Cattanaach, M. Breen, M. Binns *et al.* 2001 Canine homolog of the  
537 T-box transcription factor T; failure of the protein to bind to its DNA target leads to a  
538 short-tail phenotype. *Mamm. Genome* **12**: 212-218.

539 Herrmann, B. G., S. Labeit, A. Poustka, T. R. King, and H. Lehrach, 1990 Cloning of the T-  
540 Gene Required in Mesoderm Formation in the Mouse. *Nature* **343**: 617-622.

541 Herrmann, B. G., and A. Kispert, 1994 The T genes in embryogenesis. *Trends Genet.* **10**: 280-  
542 286.

543 Kelley, L., and M. J. E. Sternberg, 2009 Protein structure prediction on the Web: a case study  
544 using the Phyre server. *Nat. Prot.* **4**: 363-371.

545 Kispert, A., B. G. Herrmann, M. Leptin, and R. Reuter, 1994 Homologs of the Mouse  
546 Brachyury Gene Are Involved in the Specification of Posterior Terminal Structures in  
547 *Drosophila*, *Tribolium*, and *Locusta*. *Gene Dev.* **8**: 2137-2150.

548 Kispert, A., and B. G. Herrmann, 1994 Immunohistochemical Analysis of the Brachyury  
549 Protein in Wild-Type and Mutant Mouse Embryos. *Developmental Biologie* **161**: 179-  
550 193.

551 MacArthur, D., T. Manolio, D. Dimmock, H. Rehm, J. Shendure *et al.* 2014 Guidelines for  
552 investigating causality of sequence variants in human disease. *Nature* **508**: 469-476.

553 Müller, C. W., and B. G. Herrmann, 1997 Crystallographic structure of the T domain-DNA  
554 complex of the Brachyury transcription factor. *Nature* **389**: 884-888.

555 Nibu, Y., D. S. Jose-Edwards, and A. Di Gregorio, 2013 From Notochord Formation to  
556 Hereditary Chordoma: The Many Roles of Brachyury. *Biomed Res. Internat.* DOI  
557 10.1155/2013/826435.

558 Odenthal, J., P. Haffter, E. Vogelsang, M. Brand, F. J. M. vanEeden *et al.* 1996 Mutations  
559 affecting the formation of the notochord in the zebrafish, *Danio rerio*. *Development*  
560 **123**: 103-115.

561 Pennimpe, T., J. Proske, A. Koenig, J. A. Vidigal, M. Morkel *et al.* 2012 In vivo  
562 knockdown of Brachyury results in skeletal defects and urorectal malformations  
563 resembling caudal regression syndrome. *Dev. Biol.* **372**: 55-67.

564 Pillay, N., V. Plagnol, P. S. Tarpey, S. B. Lobo, N. Presneau *et al.* 2012 A common single-  
565 nucleotide variant in T is strongly associated with chordoma. *Nat. Genet.* **44**: 1185-  
566 1187.

567 Popescu, P., H. Hayes, and B. Dutrillaux, 2000 Chromosome preparation, pp. 1-24 in  
568 *Techniques in Animal Cytogenetics (Principles and Practice)*, Springer Berlin  
569 Heidelberg.

570 Postma, A. V., M. Alders, M. Sylva, C. M. Bilardo, E. Pajkrt *et al.* 2014 Mutations in the T  
571 (brachyury) gene cause a novel syndrome consisting of sacral agenesis, abnormal  
572 ossification of the vertebral bodies and a persistent notochordal canal. *J. Med. Genet.*  
573 **51**: 90-97.

574 Satoh, N., K. Tagawa, and H. Takahashi, 2012 How was the notochord born? *Evol. Dev.* **14**:  
575 56-75.

576 Searle, A. G., 1966 Curtailed, a new dominant T-allele in the house mouse. *Genet. Res.* **7**: 86-  
577 95.

578 Smith, J., 1997 Brachyury and the T-box genes. *Curr. Opin. Genet. Developm.* **7**: 474-480.

579 Thomsen, B., P. Horn, F. Panitz, E. Bendixen, A. H. Petersen *et al.* 2006 A missense  
580 mutation in the bovine SLC35A3 gene, encoding a UDP-N-acetylglucosamine  
581 transporter, causes complex vertebral malformation. *Genome Res.* **16**: 97-105.

582 Ulrich, R., A. C. Stan, M. Fehr, C. Mallig, and C. Puff, 2010 Desmoplastic ganglioglioma of  
583 the spinal cord in a western European hedgehog (*Erinaceus europaeus*). *J. Vet. Diagn.*  
584 *Invest.* **22**: 978-983.

585 van de Ven, C., M. Bialecka, R. Neijts, T. Young, J. E. Rowland *et al.* 2011 Concerted  
586 involvement of Cdx/Hox genes and Wnt signaling in morphogenesis of the caudal  
587 neural tube and cloacal derivatives from the posterior growth zone. *Development* **138**:  
588 3859.

589 Vlangos, C. N., A. N. Siuniak, D. Robinson, A. M. Chinnaiyan, R. H. Lyons *et al.* 2013  
590 Next-generation sequencing identifies the Danforth's short tail mouse mutation as a  
591 retrotransposon insertion affecting *Ptf1a* expression. *Plos Genet.* **9**: e1003205.

592 Yamaguchi, T. P., S. Takada, Y. Yoshikawa, N. Y. Wu, and A. P. McMahon, 1999 T  
593 (*Brachyury*) is a direct target of *Wnt3a* during paraxial mesoderm specification. *Gene*  
594 *Dev.* **13**: 3185-3190.

595 Yang, X. R., D. Ng, D. A. Alcorta, N. J. Liebsch, E. Sheridan *et al.* 2009 T (*brachyury*) gene  
596 duplication confers major susceptibility to familial chordoma. *Nat. Genet.* **41**: 1176-  
597 1178.

598 Zimin, A. V., A. L. Delcher, L. Florea, D. R. Kelley, M. C. Schatz *et al.* 2009 A whole-  
599 genome assembly of the domestic cow, *Bos taurus*. *Genome Biol.* **10**: R42.

600  
601

602

603 **Supporting Information**

604 **Kromik\_Genetics\_Supporting\_information\_2014\_12\_12.docx**

605

606 **File S1.** Video documentation of neurological deficit in a VSD-affected calf: non-ambulatory  
607 paraparesis

608

609

610